

# AN AUTOMATIC REGISTRATION-FUSION SCHEME BASED ON SIMILARITY MEASURES: AN APPLICATION TO DENTAL IMAGING

E. I. Zacharaki<sup>1</sup>, P. Asvestas<sup>1</sup>, G. K. Matsopoulos<sup>1</sup>, K. K. Delibasis<sup>1</sup>, and K. S. Nikita<sup>1</sup>

<sup>1</sup> Department of Electrical and Computer Engineering, National Technical University of Athens, Greece  
e-mail: ezachar@biosim.ntua.gr

**Abstract-** A novel automatic registration-fusion scheme based on similarity measures is proposed in this paper. It utilises the geometrical configuration between the X-ray source, the CCD sensor and the target tissue using the appropriate geometric transformations, as well as the calculation of similarity measures between two dental radiographic images to be registered. Moreover, a fusion process has been developed to combine information from registered dental images. Result on clinical data reveals the advantageous performance of the proposed automatic registration method compared to the manual one using an independent evaluation criterion such as the mutual information criterion. Furthermore, the automatic registration approach outperforms despite the fuzzy dental boundaries and the lack of characteristic edges of the radiographic images. These preliminary findings may be used in order to establish the use of the proposed automatic method relieving the expert from the tedious and time-consuming task of defining analogous markers between the two radiographic images.

**Keywords** – registration, affine transformation, cross-correlation, mutual information, dental X-ray images, similarity measures

## I. INTRODUCTION

CCD technology for capturing digital dental radiographs has entered routine clinical use [1]. The advantages over traditional film based imaging devices are profound, especially when considering patient X-ray dose and the possibilities of information extraction through image processing techniques. The possibility of storing a number of pre- and post-treatment digital radiographic images of the same patient imposes the problem of spatial alignment or equivalently registration of these images. By registering those dental images, the specialist can then perform any quantitative comparisons, concerning the evolution of abnormalities (cysts, tooth decay etc.) or healing processes, as well as the assessment of the effectiveness of the therapeutic scheme (implants, root canal surgery etc.). One of the most useful techniques, as well as challenging problems, is the combination, or fusion of information from two radiographic images from the same patient. A prerequisite for the image fusion is the registration, or spatial alignment of the two images, so that the same anatomical structures coincide on both images. After registration has been achieved, fusion can be used, in form of pseudocolor blending, subtraction imaging or masking between the two images to evaluate the progression of pathological conditions, such as cysts or tooth decays, or healing processes, as well as the assessment of the effectiveness of the therapeutic scheme (implants, root canal surgery etc.).

In general, different images are misaligned because of geometric distortions caused by: patient movements, imaging system geometric configurations (X-ray beam and CCD sensor in relative to the target tissue), physiological movements (respiration, heart beat) and development of abnormalities. It has been successfully applied to register CT, MRI, SPECT and PET data from [2].

The process of image registration can be formulated as a problem of optimising a function that quantifies the match between the original and the transformed image [3]. Several image features have been used for the matching process, depending on the modalities used, the specific application and the implementation of the transformation, such as markers, landmarks, surfaces or volumes of interest. Registering dental images is a tedious process since the identification of common points between the two images is sometimes a difficult task. Moreover, the lack of characteristic edges of the radiographic images cannot be used as a prerequisite for the registration, as it is successfully used in other applications [3]. Therefore, an automatic registration method is proposed in this paper for registering dental images, which does not require much user intervention.

## II. METHODOLOGY

Dental X-ray images were acquired using an X-ray dental system. The images were then digitised using a Panasonic digital camera with a CCD sensor and driven on a dedicated PC for further processing. The developed software is capable of displaying, processing and manipulating dental images. Two approaches have been developed throughout the presented paper for registering the dental images: the proposed automatic registration method and the manual approach.

### *The proposed automatic registration method*

The automatic registration method is based of a novel assembly of algorithms, which ultimately offers increased degree of automation by minimising the need for user intervention. The algorithm consists of three steps. In the first step we try to detect automatically similar quadrangular regions in the two images to be registered. We use the three of the four vertices of each region as pairs of homologous points. In the second step, we apply a global geometric transformation to register these corresponding anatomical points, whereas in the last step, the calculated parameters of the geometric transformation are used as starting estimates for a global registration using optimisation techniques.

### A. Determination of homologous regions

The system utilises the properties of the spatial frequency domain to locate regions  $B_i$  of strong edge presence. For each one of these regions in the unregistered image  $I_F(x, y)$ , a local rigid transformation,  $T_i: B_i \rightarrow \mathbb{R}^2$ , is calculated by maximising a similarity criterion between the region  $B_i$  and a corresponding region in the reference image  $I_R(x, y)$ . The following three intensity-based similarity measures are investigated:

#### a) Normalised cross-correlation coefficient

$$CC = \frac{\sum [I_F(x, y) - \bar{I}_F][I_R(T_i(x, y)) - \bar{I}_R]}{\sqrt{\sum_{(x,y) \in B_i} [I_F(x, y) - \bar{I}_F]^2} \sqrt{\sum_{(x,y) \in B_i} [I_R(T_i(x, y)) - \bar{I}_R]^2}} \quad (1)$$

where  $\bar{I}_F$  and  $\bar{I}_R$  are the mean values of the images  $I_F$  and  $I_R$  in the regions  $B_i$  and  $T(B_i)$ , respectively.

#### b) Gradient correlation

Gradient images  $dI/di$  and  $dI/dj$ ,  $I = I_F$  or  $I_R$ , representing the derivative in the two orthogonal axes ( $i, j$ ) of the image are created using horizontal and vertical Sobel templates. The gradient correlation is the average of the normalised cross-correlations between  $dI_F/di$  and  $dI_R/di$  and between  $dI_F/dj$  and  $dI_R/dj$  [4].

#### c) Mutual information

$$MI = \sum_{k=0}^{G-1} \sum_{l=0}^{G-1} p_{I_F I_R}(k, l) \log_2 \frac{p_{I_F I_R}(k, l)}{p_{I_F}(k) p_{I_R}(l)} \quad (2)$$

where  $0 \dots G-1$  is the intensity range,  $p_{I_F I_R}(k, l)$  is the joint probability distribution and  $p_{I_F}(k)$ ,  $p_{I_R}(l)$  are the probability distributions in the regions  $B_i$  and  $T(B_i)$  of the individual images, respectively.

The multidimensional maximisation of the selected similarity measure is achieved using a local optimisation process such as the Downhill Simplex Method [5]. If the calculated maximum function value is higher than a predetermined threshold, then the similarity between the two regions is high enough, so that the three vertices of each region can be used as pairs of homologous points.

### B. Global geometric transformation

Closed form optimisation techniques [5] are subsequently applied to obtain a global geometric transformation, based on the relative positions of the similar regions that have been established in the previous step of the algorithm. The selected geometric transformation is the affine transformation [6]:

$$\begin{pmatrix} x' \\ y' \end{pmatrix} = \begin{pmatrix} a_1 & a_2 \\ b_1 & b_2 \end{pmatrix} \times \begin{pmatrix} x \\ y \end{pmatrix} + \begin{pmatrix} dx \\ dy \end{pmatrix} \quad (3)$$

where  $(x, y)$  are the initial coordinates of the homologous points,  $(a_i, b_i)$ ,  $i = 1, 2$  and  $dx, dy$  are the six parameters of the affine transformation. The parameters of the transformation are calculated by applying the Least Squares minimisation method in conjunction with Singular Value Decomposition [7].

### C. Global refine transformation

The accuracy of the registration can be improved by maximising the cross-correlation of the registered and the reference dental image using Powell's optimisation method with initial starting point the vector of the previous estimated parameters. Powell's method is a suitable optimiser, as it benefits strongly from good starting conditions.

### The manual approach

In the case of dental X-ray images, which do not exhibit strong edges, the manual approach to the image registration problem is the use of landmarks, homologous pairs of points on both images, which are placed on the images to be registered by the expert by means of software. The selected geometric transformation is the affine transformation. To compute the parameters of the affine transformation, three pairs of homologous points are sufficient. In this approach, we use five pairs, which are enough to achieve robustness of the transformation. The parameters of the affine transformation are calculated by applying the Least Squares minimisation method in conjunction with Singular Value Decomposition [7], as the number of user defined landmarks is greater than the number of independent parameters of the transformation.

### Fusion Process

A fusion process is developed and applied after the performance of the registration process. The fusion process is based on modelling the binary joint histogram of the reference and corresponding transformed dental image and the utilisation of pseudocolor encoding and blending approaches [8]. The differences between the reference image  $I_R$  and the image to be registered  $I_F$  can be considered as the effect of a system, which gets as input the image  $I_R$  and produces the image  $I_F$ . This system consists of three levels, as shown in Fig. 1. In the first level,  $T_{anat}$ , the anatomical differences between the two images are produced, in the second level,  $T_{geom}$ , the images are registered in terms of geometrical alignment and in the third level,  $T_{gray}$ , the differences in intensity are eliminated. As long as the geometrical transformation  $T_{geom}$  and the intensity transformation  $T_{gray}$  are computed, the demonstration of the anatomical differences is processed as follows. Image  $I_F$  is fed to a system, of which the first two levels are the inverse

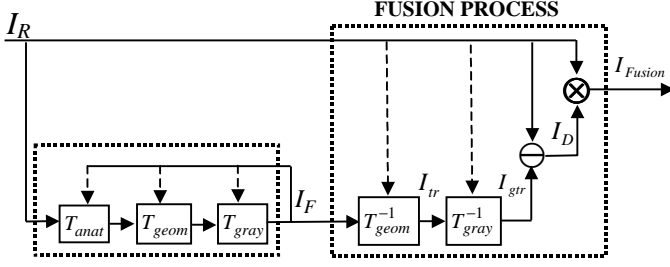


Fig 1. Flow diagram of the fusion process

transformations  $T_{geom}^{-1}$  and  $T_{gray}^{-1}$ . The image after the intensity transformation  $I_{gr}(x, y)$  is produced according to the equation

$$I_{gr}(x, y) = aI_{tr}(x, y) + \sum_{k=1}^N b_k B_k(x, y) \quad (4)$$

where  $I_{tr}(x, y)$  is the geometric transformed image. The parameter  $a$  models the different contrast between the two images, while the term  $\sum_{k=1}^N b_k B_k(x, y)$  is used to model differences in the brightness of the images or gradient intensities using appropriate functions  $B_k(x, y)$ . The number of pixels with anatomical differences between the reference image and the image  $I_{gr}$  is small enough to be able to consider  $I_{gr}(x, y) \approx I_R(x, y)$ . Thus, the parameters of the intensity transformation can be calculated by minimising the square error of the difference between these two images. Image  $I_{gr}$  is then subtracted from the reference image. A masking processes between the image of the difference  $I_D$  and the reference image  $I_R$  with output the fused image  $I_{Fusion}$ :

$$I_{Fusion} = \begin{cases} I_R(x, y), & \text{if } I_D(x, y) < \text{Threshold} \\ \infty I_D(x, y) & \text{if } I_D(x, y) \geq \text{Threshold} \end{cases} \quad (5)$$

A colour map is created to indicate the size of the difference, in order to distinguish the noise from any pathological dissimilarity. A threshold, definable by the user at the time of the execution, is inserted, in order to make visible regions only with high values in the image  $I_D$ . Thus, the visibility of the fused image is optimally enhanced.

### III. RESULTS

Experimental results are obtained by applying the automatic registration method in comparison with the manual one. In both cases, the fusion process has been applied in order to evaluate the performance of the two registration methods, as shown in the following figures. In the Fig. 2(a) and (b), the test image (left) and the reference image (right) are displayed. The transformed image is

displayed after the automatic registration process in Fig. 2(c) and after the manual approach in Fig. 2(e). In the automatic registration process the normalised cross-correlation coefficient was used as similarity measure. Finally, in Fig. 2(d) and 2(f), the fusion of the difference between the reference and transformed image each time is displayed in pseudocolour (shown as dark grey areas), whereas the rest of the reference image remains unchanged.

Comparing Fig. 2(d) and 2(f), it is obvious that the automatic registration method using the cross-correlation

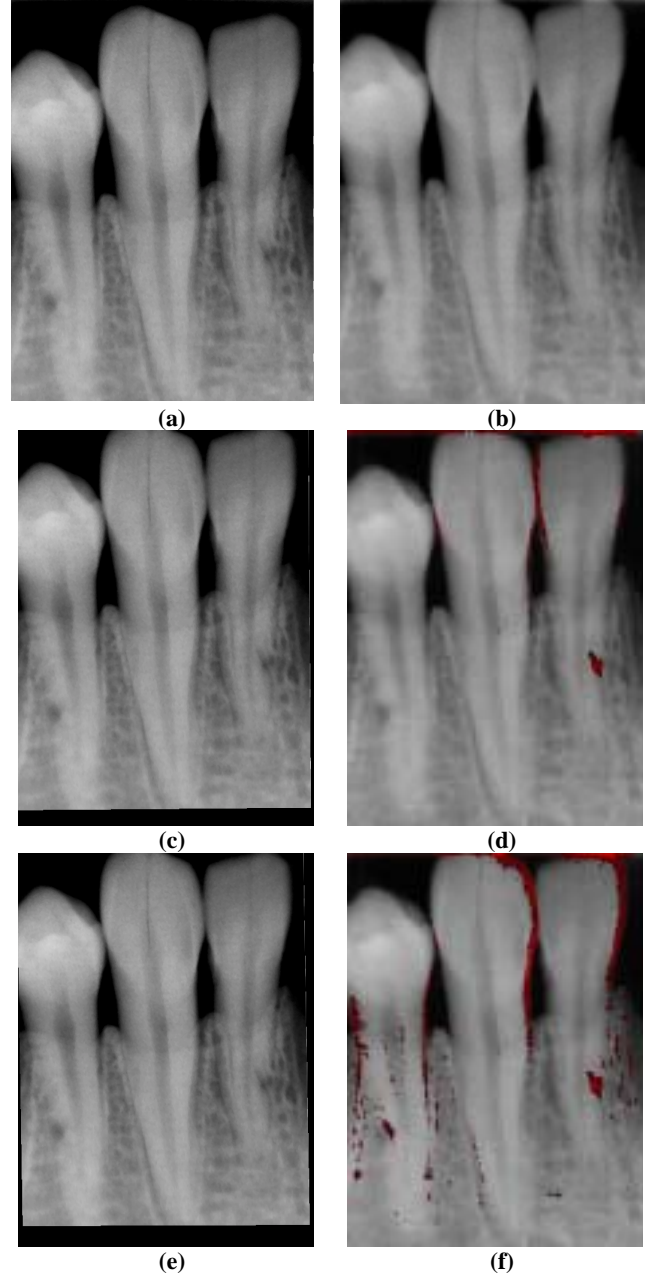


Fig. 2. Performance of the proposed automatic and the manual registration and fusion scheme on dental images. (a) image to be registered, (b) reference image, (c) –(d) automatic registered and fused image and (e)–(f) manual registered and fused image.

criterion outperforms comparing to the manual method, since the areas of differences are more evident in the manual fused image. These findings are explained by the fact that the manual method performs locally to the areas where the expert places points of correspondence. The points were placed on the half top of the image, since only there existed characteristic edges. Thus, the manual registration failed at the bottom of the image. On the other hand, the fusion result presented in Fig. 2(d) shows almost only a dark grey area in the produced cavity, which is expected according to the test procedure.

Furthermore, a quantitative analysis of the study has been performed. Initially, the performance of the automatic method was tested against the most accurate similarity criterion. For this purpose, the following three criteria have been tested: the normalised cross-correlation coefficient, the gradient correlation and the mutual information. An independent measure of match is employed in order to evaluate these similarity criteria, such as the average distance, between the selected pairs of points:

$$D_{ave} = \frac{1}{n} \sum_{i=1}^n \|T(x_{i1}, y_{i1}) - (x_{i2}, y_{i2})\| \quad (6)$$

where  $(x_{i1}, y_{i1}), (x_{i2}, y_{i2})$  ( $i = 1, 2, \dots, n$ ) represent the pairs of the user-defined markers,  $T(x, y)$  stands for the selected geometric transformation and  $\|\bullet\|$  denotes the Euclidean distance [6]; the smaller the distance, the better the registration achieved. In Table I, the ratio of the average distance of the automatic registration method to the average distance of the manual registration, using each criterion is presented. It is evident that the cross-correlation similarity criterion has performed significantly better than the two other proposed similarity measures. Therefore, in order to determine the homologous regions of the automatic method, the cross-correlation coefficient was finally chosen.

Furthermore, a quantitative analysis was performed in order to compare the two registration methods: the proposed automatic against the manual. These results are shown in Table II. It must be pointed out that the comparison of the two methods has been achieved using an independent measure of match, so as our results to be unbiased.

TABLE I  
PERFORMANCE OF THE AUTOMATIC REGISTRATION METHOD IN TERMS OF THEIR SIMILARITY CRITERIA: CROSS-CORRELATION, GRADIENT CORRELATION, MUTUAL INFORMATION. THE NUMBERS CORRESPOND TO THE RATIO OF AVERAGE DISTANCE AUTOMATIC/ MANUAL

Pairs	Cross-Correlation	Gradient Correlation	Mutual Information
1	1.442	1.435	1.479
2	2.247	2.570	1.804
3	1.216	1.335	1.329
4	3.000	3.614	3.671
5	1.199	1.372	1.498
6	1.259	1.355	1.539
7	2.668	2.298	2.528
8	2.172	2.734	2.396
9	2.453	2.463	2.361
Mean Value	1.962	2.131	2.067

TABLE II  
COMPARISON OF THE AUTOMATIC REGISTRATION METHOD AGAINST THE MANUAL ONE, IN TERMS OF MUTUAL INFORMATION CRITERION

Pairs	Manual Registration	Automatic Registration
1	2.493	2.852
2	1.912	1.923
3	2.296	2.598
4	2.101	2.660
5	2.257	2.713
6	1.984	2.175
7	1.302	1.501
8	1.290	1.373
9	1.964	2.745
Mean Value	1.955	2.282

It is evident that the automatic registration, using the cross-correlation, as a similarity criterion, consistently and substantially outperformed the manual registration for all pairs.

#### IV. CONCLUSION

A novel automatic registration and fusion scheme was presented in this paper. The scheme is applied on X-ray dental images. The overall performance of the scheme is limited up to 40 sec for dental images with size of 494x660 pixels on a common PC. The results have shown the advantageous performance of the automatic registration method against the manual one, both qualitative and quantitative, using similarity measures. The final fused image records any pathological dissimilarity between the two dental images, thus assessing the effectiveness of any therapeutic scheme applied. Further evaluation of the proposed registration and fusion scheme is necessary in order to be incorporated as a routine examination on a clinical setting.

#### REFERENCES

- [1] S. Eikenberg, R. Vandre, "Comparison of digital dental X-ray systems with self-developing film and manual processing for endodontic file length determination," *J Endod*, vol. 26, no. 2, pp. 65-7, 2000.
- [2] P.A. Van den Elsen, E.J. Pol, and M.A. Viergever, "Medical image matching: A review with classification," *IEEE Eng. In Medicine and Biology*, vol. 12, no. 1, pp. 26-39, 1993.
- [3] G.K. Matsopoulos, N.A. Mouravliansky, K.K. Delibasis, and K.S. Nikita, "Automatic Registration of Retinal Images with Global Optimization techniques," *IEEE Trans. Information Technology in Bio-engineering*, vol. 3, pp. 47-60, 1999.
- [4] G.P. Penney, J. Weese, J.A. Little, P. Desmedt, D.L. G. Hill, and D.J. Hawkes, "A Comparison of Similarity Measures for Use in 2-D-3-D Medical Image Registration," *IEEE Trans. on Medical Imaging*, vol. 17, no. 4, pp.586-595, 1998.
- [5] W. Press, B. Flannery, S. Teukolsky, and W. Vetterling, *Numerical recipes in C*, Cambridge University Press, 1992.
- [6] C. Fuh, and P. Maragos, "Motion displacement estimation using an affine model for image matching," *Optical Engineering*, vol. 30, pp. 881-887, 1991.
- [7] K.S. Arun, T.S. Huang and S. Blostein, "Least-squares fitting of two 3-D sets," *IEEE Trans. PAMI*, vol. 9, no. 5, pp. 698-700, 1987.
- [8] R. Rezaee, C. Nyqvist, P. van der Zwet, E. Jansen, and J. Reiber, "Segmentation of MR images by a fuzzy C-Means algorithm," *Comput. Cardiology*, pp. 21-24, 1995.